Membrane currents and the resting membrane potential in cultured bovine pulmonary artery endothelial cells

Thomas Voets, Guy Droogmans and Bernd Nilius

Laboratory of Physiology, Catholic University of Leuven, Campus Gasthuisberg, B-3000 Leuven, Belgium

1. We have used the whole-cell patch-clamp technique to characterize the ionic conductances that determine the resting membrane potential in cultured endothelial cells from calf pulmonary artery (CPAE cells).

2. Resting membrane potentials were scattered between −88 and +5 mV with a mean ± S.E.M. of −26 ± 3 mV ($n = 104$).

3. The most prominent membrane current in resting cells was an inwardly rectifying K^+ current. This current showed Na^+-dependent inactivation and was efficiently blocked by external Ba^{2+} ($EC_{50} = 2{\cdot}2$ μM), but was relatively insensitive to quinine, quinidine and TEA.

4. Hypertonic cell shrinkage inhibited an outwardly rectifying Cl^- current, which was also efficiently blocked by 5-nitro-2-(3-phenylpropylamino)-benzoate (NPPB; 100 μM), quinine (500 μM) and quinidine (500 μM).

5. A linear, time-independent background current remained after elimination of these two currents. This current was dependent on extracellular monovalent cations with a permeability sequence of $Cs^+ > Na^+ > Li^+ \gg$ *N*-methyl-D-glucamine. It was partially blocked by millimolar concentrations of the divalent cations Ca^{2+}, Ni^{2+} and Ba^{2+}. Gd^{3+} (200 μM) had no significant effect on this background current.

6. Continuous measurements of the membrane potential confirm that the three described conductances are the major determinants of the membrane potential. Due to the low slope conductance in the region between −70 and 0 mV, small changes in one of the current components can evoke large depolarizations or hyperpolarizations, which explains the large scattering of the resting membrane potentials.

The membrane potential is an important regulator of intra- and intercellular signal transduction in various vascular functions. In vascular endothelium, it contributes to the driving force for Ca^{2+} and thus regulates the calcium-dependent release of vasoactive compounds from the endothelial cells (Adams, Barakeh, Laskey & van Breemen, 1989; Cannell & Sage, 1989; Graier, Sturek & Kukovetz, 1994). It has also been shown that endothelium and vascular smooth muscle are coupled via myo-endothelial gap junctions (Rhodin, 1967; Davies, Olesen, Clapham, Morrel & Schoen, 1988). Therefore a direct influence of the endothelial membrane potential on the membrane potential and the contractile state of vascular smooth muscle is now widely accepted (Davies *et al.* 1988; Daut, Standen & Nelson, 1994; Beny & Pacicca, 1994). Furthermore, changes in membrane potential during the cell cycle, including a hyperpolarization during the G_1–S phase transition have been observed in several types of proliferating cells, indicating that the control of the membrane potential is an essential requirement in growing cells (Kiefer, Blume & Kaback, 1980; Boonstra, Mummery, Tertoolen, van der Saag & De Laat, 1981; Wonderlin, Woodfork & Strobl, 1995).

The aim of this study was to identify the different conductances that regulate the membrane potential in resting macrovascular endothelial cells from bovine pulmonary artery (CPAE). Most electrophysiological studies on resting endothelial cells focus on the very prominent inwardly rectifying K^+ current (Nilius, Schwarz & Droogmans, 1993; Fransen, Demolder & Brutsaert, 1995; von Beckerath, Dittrich, Klieber & Daut, 1996). Yet it seems that other conductances are present under control conditions, as measured membrane potentials often deviate largely from the theoretical equilibrium potential for K^+. Here we show that at least three current types exist in resting CPAE cells: an inwardly rectifying K^+ current, a volume-sensitive Cl^- current and a non-selective cation current. The resting membrane potential is determined by an interplay of these currents.

METHODS

Cells

We used single endothelial cells from an established cell line from calf pulmonary artery (cell line CPAE; American Type Culture Collection, Rockville, MD, USA). Cells were grown in Dulbecco's modified Eagle's medium (Life Technologies, Gibco) with 20% fetal calf serum, 2 mM L-glutamine, 100 mg ml^{-1} streptomycin and 100 mg ml^{-1} penicillin. They were then detached by exposure to 0·05% trypsin in a Ca^{2+}- and Mg^{2+}-free solution, reseeded on gelatin-coated coverslips, and kept in culture for 2–4 days before use. Only non-confluent cells were used.

Electrophysiological recordings

The whole-cell mode of the patch-clamp technique was used to measure membrane potentials and membrane currents. Resting membrane potentials were continuously recorded in current-clamp mode or estimated as the zero current level in voltage-clamp mode. In general, both methods gave similar results (difference < 2 mV). Whole-cell currents were monitored with an EPC-7 (List Electronic) patch-clamp amplifier and sampled at 4 ms intervals (2048 points per record, filtered at 100 Hz). Holding potential was 0 mV. We used the following voltage protocols: (a) 400 ms lasting steps ranging from +100 to −150 mV and spaced by 25 mV (step protocol) and (b) a step to −80 mV for 0·6 s, followed by a step to −150 mV for 0·2 s and a 2·6 s linear voltage ramp to +100 mV (ramp protocol). Cell surface area was estimated from the cell capacitance, as indicated by the analog compensation circuit of the EPC-7 amplifier, and by assuming a specific capacitance of 1 $\mu F\ cm^{-2}$.

Experiments were performed at room temperature (20–23 °C). Pooled data are given as means ± S.E.M. Significance was tested at $P = 0{\cdot}05$ using Student's paired or unpaired t tests.

Solutions

The standard extracellular solution was a Krebs solution, containing (mM): 150 NaCl, 6 KCl, 1 $MgCl_2$, 1·5 $CaCl_2$, 10 glucose and 10 Hepes; pH 7·4 with NaOH. To examine cation selectivity, we used Krebs solutions in which Na^+ was partly or fully replaced by Cs^+, Li^+ or *N*-methyl-D-glucamine ($NMDG^+$). The osmolality of these solutions, as measured with a vapour osmometer (Wescor 5500, Schlag, Gladbach, Germany) was 320 ± 5 mosmol kg^{-1}. Hypertonicity was obtained by addition of 100 mM mannitol, resulting in an osmolality of 410 ± 5 mosmol kg^{-1}. The normal pipette solution contained (mM): 40 KCl, 100 potassium aspartate,

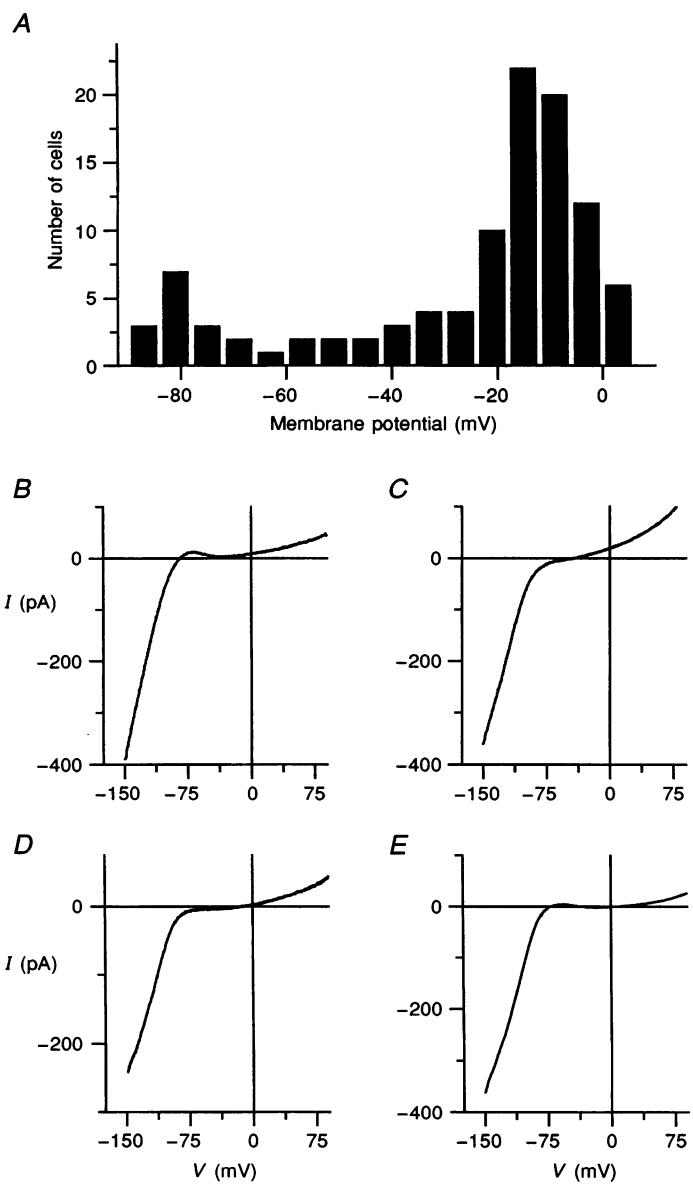

Figure 1. Membrane potentials in resting endothelial cells

A, membrane potentials measured immediately after establishing the whole-cell configuration ($n = 104$). The histogram was constructed with a bin width of 6 mV. *B–E*, current–voltage relations measured during the ramp protocol in normal Krebs external solution from a hyperpolarized cell (−82 mV; *B*), an intermediately polarized cell (−52 mV; *C*), a depolarized cell (−12 mV; *D*) and a cell with three zero current potentials (−72, −40 and 0 mV; *E*).

1 $MgCl_2$, 0·5 EGTA, 4 Na_2ATP and 10 Hepes; pH 7·2 with KOH. In some experiments K^+ was replaced by $NMDG^+$ or Cs^+. Pipette solutions with 5 mM BAPTA instead of 0·5 mM EGTA were sometimes used to buffer intracellular Ca^{2+}. A low-Cl^- pipette solution was also used, in which KCl was partially (30 mM) replaced by potassium aspartate. Stock solutions of quinine hydrochloride, quinidine hydrochloride monohydrate (Sigma) and 5-nitro-2-(3-phenylpropylamino)-benzoate (NPPB; Research Biochemicals International) were made in DMSO (final DMSO concentration < 0·1 %).

RESULTS

Distribution of resting membrane potentials

Membrane potentials ranged from −88 to +5 mV with a mean of −26 ± 3 mV ($n = 104$; Fig. 1*A*). The cells could be roughly divided into three classes according to their membrane potential: hyperpolarized (< −70 mV, 13% of the cells), intermediately polarized (between −70 and −30 mV, 14%) and depolarized (> −30 mV, 69%). Current–voltage relations for cells from each of the three classes are shown in Fig. 1*B–D*. The current–voltage relations of the remaining cells (4/104) crossed the zero current level at three potentials (Fig. 1*E*). The membrane potential measured in current clamp in these cells depended on the holding potential that was applied before switching to current-clamp mode, with hyperpolarizing holding potentials yielding hyperpolarized membrane potentials and vice versa. Due to the low incidence of these cells (<4%), we did not study this phenomenon of bi-stability (see Mehrke, Pohl & Daut, 1991) in more detail.

Separation of current components

Two procedures were used to dissect the total membrane current of resting cells into its various components: (a) addition of 100 μM Ba^{2+} to the external solution and (b) cell shrinkage induced by addition of 100 mM mannitol. The rationale for these protocols was to block inwardly rectifying K^+ currents and volume-sensitive Cl^- currents, respectively. Figure 2*A* shows current–voltage relations recorded from a cell before and after these treatments. The Ba^{2+}-sensitive current (Fig. 2*B*) showed strong inward rectification and reversed at −83 ± 1 mV ($n = 10$). The shrinkage-sensitive current (Fig. 2*C*) showed outward rectification and reversed at −25 ± 4 mV ($n = 10$). The

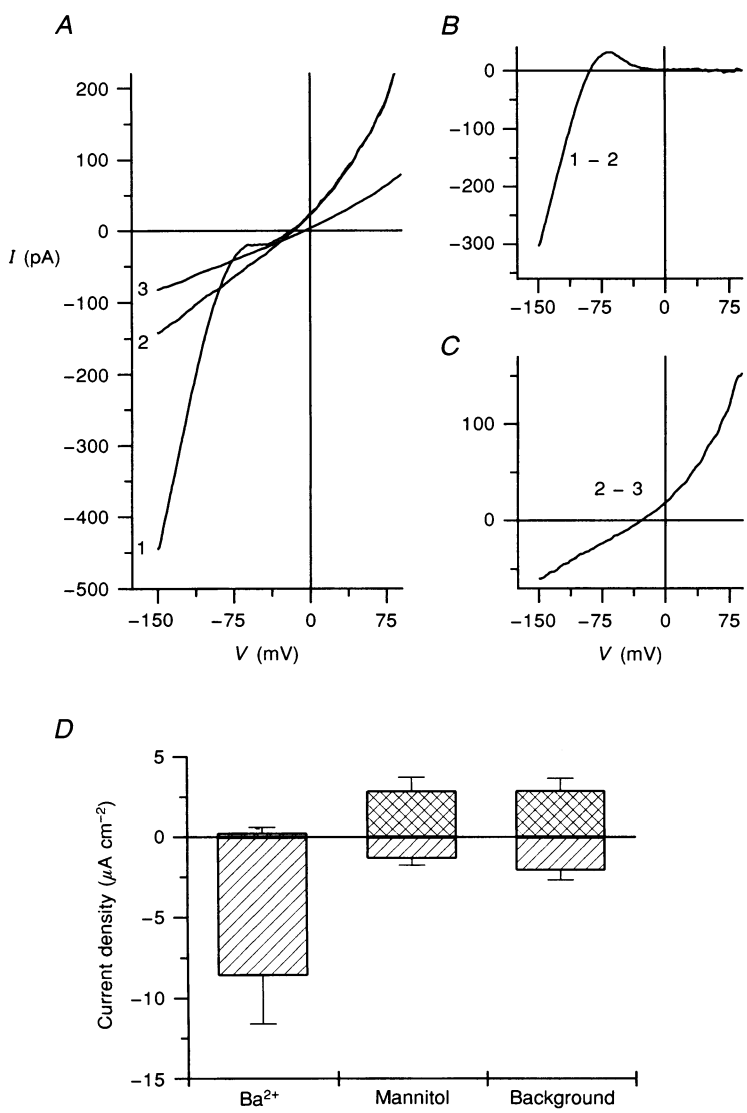

Figure 2. Dissection of different current components

A, current–voltage relations measured from a cell in normal Krebs solution (trace 1) and in a Krebs solution supplemented with 100 μM Ba^{2+} (trace 2) or 100 μM Ba^{2+} and 100 mM mannitol (trace 3). *B*, current inhibited by Ba^{2+}. *C*, current inhibited by hypertonicity. *D*, the amplitudes of the Ba^{2+}-sensitive current, the hypertonicity-sensitive current and the remaining background current in 10 cells were measured at ±100 mV and normalized to membrane surface area.

current–voltage relation remaining after applying both treatments (trace 3 in Fig. 2*A*) was almost linear and reversed at -1 ± 3 mV ($n = 10$). The magnitudes of these three current components expressed per unit of membrane capacitance and measured at −100 and +100 mV are summarized in Fig. 2*E*.

Inwardly rectifying K^+ currents

The inwardly rectifying component strongly increased when the extracellular K^+ concentration was increased from 6 mM to 15, 30, 60 or 120 mM (Fig. 3*A*). Its maximal slope conductance was proportional to the square root of the K^+ concentration (Fig. 3*B*), which is typical for currents through inwardly rectifying K^+ channels (Hille, 1992). Currents during hyperpolarizing steps to −125 mV and −150 mV showed a time- and voltage-dependent inactivation inducing the typical crossing over of the currents. This inactivation disappeared almost completely when extracellular Na^+ was replaced by $NMDG^+$, whereas 100 μM Ba^{2+} caused a fast and almost complete block (Fig. 3*C*). The EC_{50} value for the steady-state inhibition of inwardly rectifying K^+ currents by Ba^{2+}, measured at −125 mV, was 2·2 μM ($n = 5$) (data not shown). Quinidine and quinine (1 mM), two drugs that have been used to distinguish between different types of inwardly rectifying K^+ channels, had only small effects on the inward currents (Fig. 3*D–E*). Tetraethylammonium (TEA; 10 mM), another frequently used K^+ channel blocker, caused approximately 30% inhibition at −125 mV.

Volume-sensitive Cl^- currents

In order to investigate other current components, inwardly rectifying K^+ currents were eliminated by addition of 100 μM Ba^{2+} or by removal of extracellular KCl. The remaining current showed outward rectification. Reducing the extracellular Cl^- concentration from 155 mM to 40 and 5 mM (NaCl partially or fully replaced by sodium gluconate) under these conditions clearly decreased the outward

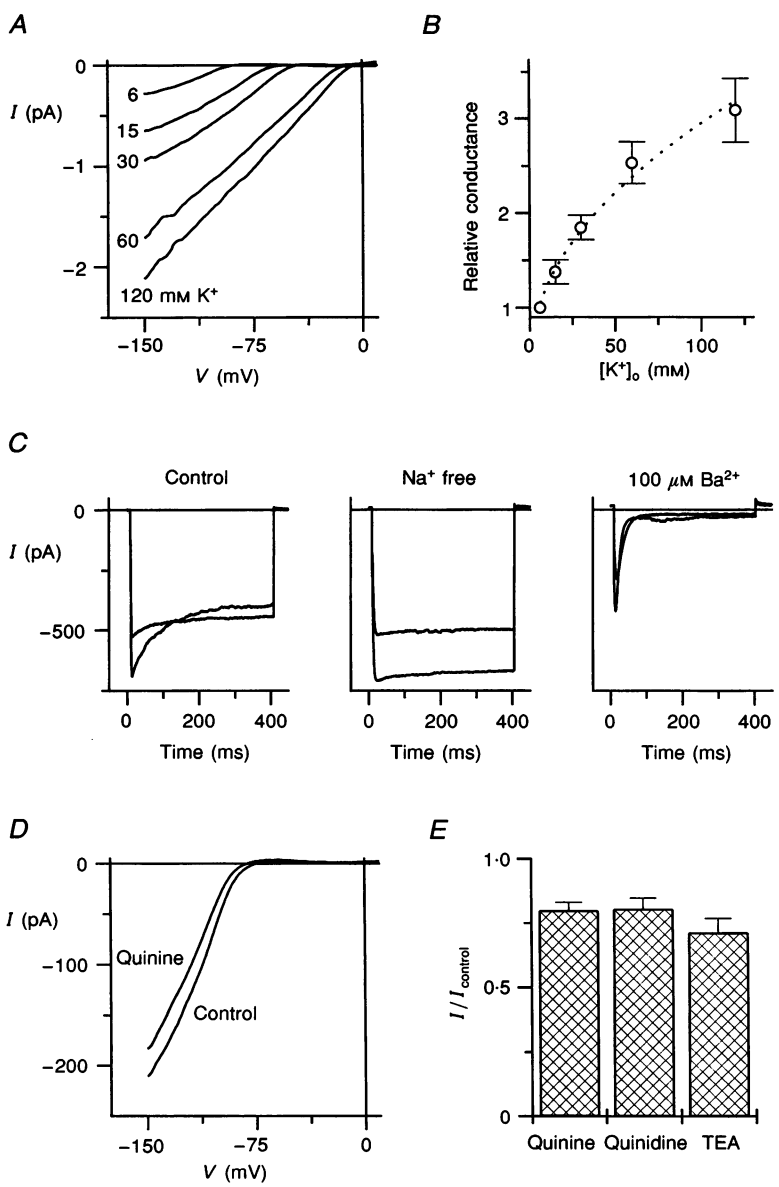

Figure 3. Inwardly rectifying K^+ currents

A, current–voltage relations measured from a cell in normal Krebs solution (6 mM K^+) and in Krebs solution with 15, 30, 60 and 120 mM K^+ (NaCl partially replaced by KCl). *B*, the maximal slope conductance of the inward currents with the different extracellular K^+ concentrations was normalized to that in normal Krebs solution and the data points were fitted by a square root function ($n = 3$). *C*, currents measured in response to voltage steps to −125 and −150 mV in normal Krebs solution (left), Na^+-free Krebs solution (middle) and in Na^+-free Krebs solution with 100 μM Ba^{2+} (right). *D*, currents measured in normal Krebs solution with or without 1 mM quinine. *E*, effect of 1 mM quinine, 1 mM quinidine and 10 mM TEA on inwardly rectifying K^+ currents measured at −125 mV ($n = 4$ for each drug).

current amplitude and shifted the reversal potential to more positive potentials by 16 ± 5 mV and 26 ± 5 mV ($n = 5$), respectively (Fig. 4*A*). The effect of external Cl^- replacement and the outward rectification were both absent in cells shrunken by hypertonicity (Fig. 4*B*). These findings indicate that a basal volume-sensitive anion current is present in CPAE cells under isotonic conditions, through channels that are more permeable to Cl^- than to gluconate. NPPB, a drug that efficiently blocks volume-activated Cl^- currents in endothelium ($EC_{50} = 29$ μM) (Nilius, Sehrer & Droogmans, 1994), also completely blocked the volume-sensitive current in resting endothelial cells at a concentration of 100 μM (Fig. 4*C–D*). Quinine and quinidine (500 μM) had similar blocking effects (data not shown). The current inhibited by cell shrinkage (Fig. 2*C*) or by treatment with the above-mentioned drugs (Fig. 4*D*) reversed at -25 ± 4 mV ($n = 18$), which differs from the theoretical equilibrium potential for Cl^- (−33·5 mV). However, if we assume that the relative permeability of this pathway for aspartate is the same as that of the volume-activated Cl^- current in CPAE cells ($P_{asp}/P_{Cl} = 0{\cdot}13$; the authors' unpublished results), the theoretical reversal potential for this anion permeable pathway can be calculated as −26 mV, which is in accordance with the experimental results.

Background currents

Figure 5*A* shows current traces recorded in response to 400 ms steps to potentials between −150 and +100 mV from a cell in K^+-free, hypertonic solution (to eliminate both the inwardly rectifying K^+ current and the volume-sensitive Cl^- current). This background current showed no time-dependent activation or inactivation. Replacement of extracellular Na^+ by $NMDG^+$ markedly reduced inward currents but did not affect outward currents (Fig. 5*B*). Current–voltage relations derived from the currents measured at the end of the voltage steps in the presence and absence of Na^+ are shown in Fig. 5*C*. Replacement by $NMDG^+$ induces a significant decrease of the inward current and a shift of the reversal potential towards more negative values. If we assume that the permeability of the cell membrane to $NMDG^+$ is negligible, then the difference between currents measured in Na^+ solution and $NMDG^+$ solution represents net Na^+ influx (Fig. 5*D*). The difference curve could be well fitted by the Goldman–Hodgkin–Katz relation, assuming independence of ionic movements:

$$I_S = -\left(\frac{Pz^2FE}{RT}\right)\left(\frac{[S]_o \exp(zEF/RT)}{1 - \exp(zEF/RT)}\right), \quad (1)$$

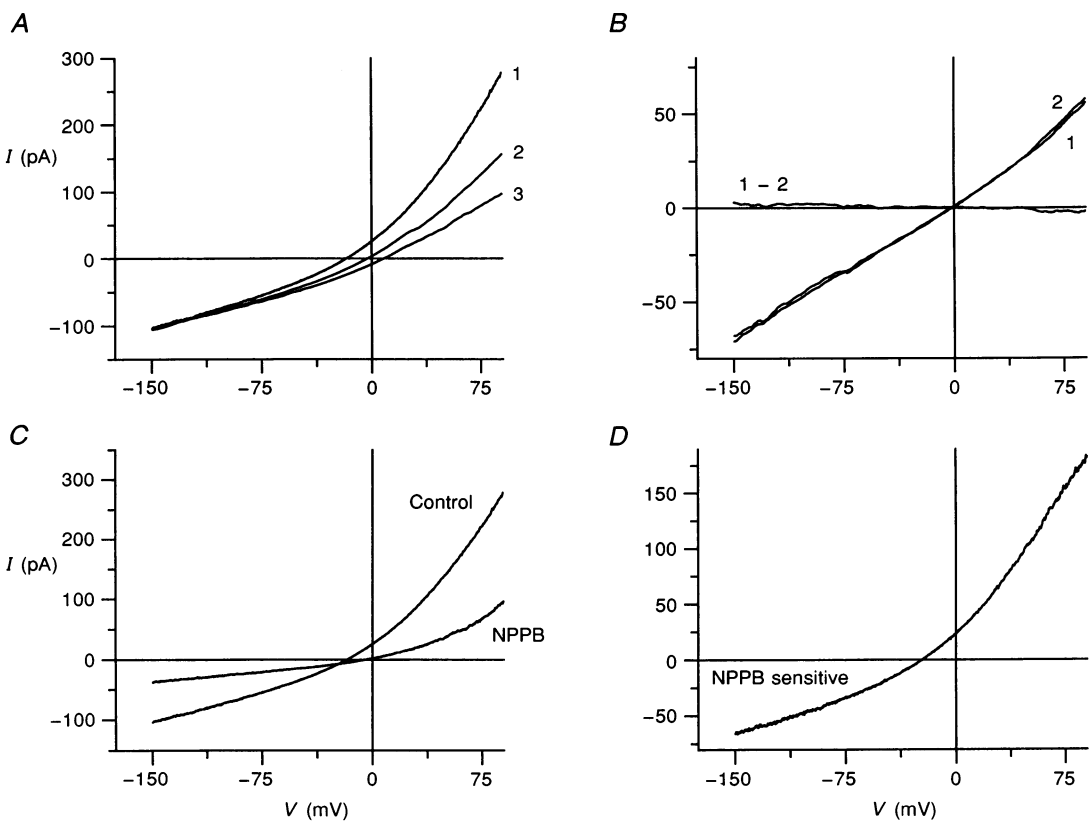

Figure 4. Volume-sensitive Cl^- currents

A, current–voltage relations measured in K^+-free Krebs solution with 155 mM (trace 1), 40 mM (trace 2) or 5 mM (trace 3) extracellular Cl^- (NaCl partially or fully replaced by sodium gluconate). *B*, currents measured in hypertonic K^+-free Krebs solution with 155 mM (trace 1) or 5 mM (trace 2) extracellular Cl^- (same cell as in *A*). *C*, currents measured in K^+-free Krebs solution with or without 100 μM NPPB. *D*, the NPPB-sensitive current reverses at −25 mV.

where I_S is the inward current per unit membrane surface area, P is the permeability constant, $[S]_o$ is the external concentration of the permeating ion and E, z, F, R and T have their usual meanings. To examine its Na^+ dependence further, the current was measured at various external Na^+ concentrations (Fig. 6*A*). The difference between current–voltage relations measured in Na^+-containing and Na^+-free solutions (Fig. 6*B*) represents the voltage dependence of the inward Na^+ current component at various external Na^+ concentrations. Figure 6*C* shows the relationship between normalized currents at different potentials and extracellular Na^+ concentration. The data points were fitted with a straight line through the origin, as predicted by eqn (1). The permeability constant for Na^+ was calculated as $(1{\cdot}01 \pm 0{\cdot}05) \times 10^{-6}$ cm s^{-1}.

Figure 7*A* shows an experiment in which extracellular Na^+ was replaced by Cs^+, Li^+ or $NMDG^+$. The current amplitudes at negative potentials, as well as the shifts in reversal potential suggest a permeability sequence $Cs^+ > Na^+ > Li^+ \gg NMDG^+$. The difference curves (Fig. 7*B*) could be fitted by eqn (1) and we obtained relative permeability coefficients for Cs^+/Na^+ and Li^+/Na^+ of $1{\cdot}28 \pm 0{\cdot}09$ and $0{\cdot}84 \pm 0{\cdot}05$, respectively ($n = 6$), corresponding to Eisenman's sequences I–IV (Hille, 1992). We could not obtain reliable permeabilities for K^+ ions because a complete block of the inwardly rectifying K^+ currents in high-K^+ extracellular solution required millimolar concentrations of Ba^{2+}, which, as will be shown below, have important blocking effects on the cation currents.

In order to investigate if outward currents measured under these conditions occur through a similar non-selective cation conductance pathway, we replaced intracellular K^+ ions by Cs^+ (Fig. 8*A*) or $NMDG^+$ (Fig. 8*B*). Currents measured with internal Cs^+ were not significantly different from those measured with internal K^+, whereas outward currents measured with internal $NMDG^+$ were more than 50% smaller (Fig. 8*C*), indicating that the outward current occurs at least partially through a conductance pathway that is equally permeable to K^+ and Cs^+, but significantly less permeable to $NMDG^+$.

We tested the effect on the background current of the divalent cations Ni^{2+}, Ba^{2+} and Ca^{2+} and of the trivalent cation Gd^{3+}. Perfusion with 2 mM Ni^{2+}- (Fig. 9*A*) or Ba^{2+}-containing (Fig. 9*B*) solutions caused a fast, voltage-

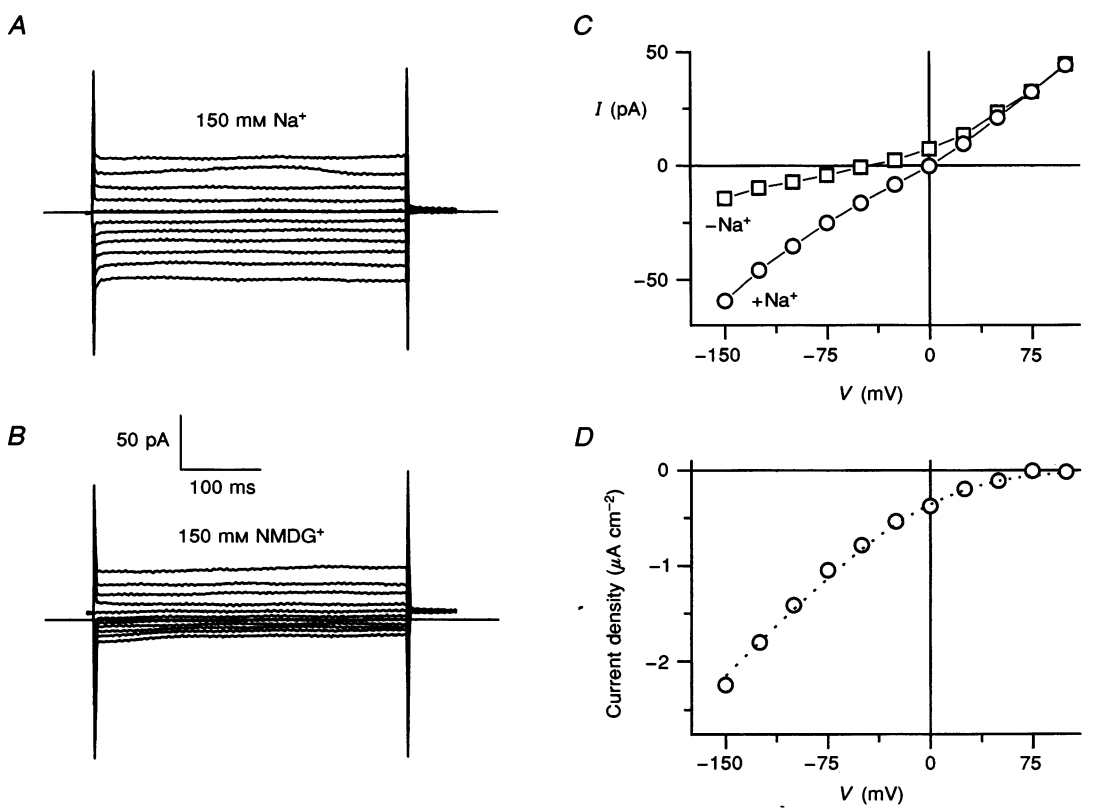

Figure 5. The background current is Na^+ dependent

A, currents measured in K^+-free hypertonic Krebs solution in response to voltage steps between −150 and 100 mV. *B*, same as *A* but with extracellular Na^+ replaced by $NMDG^+$. *C*, current–voltage relation in Na^+-containing (○) and Na^+-free (□) solution. Currents were measured at the end of the voltage steps in *A* and *B*. *D*, current–voltage relation obtained by subtracting currents measured in Na^+-free solution from those measured in Na^+-containing solution and normalizing to membrane surface area. The dotted line represents the best fit through the data points using eqn (1).

independent and fully reversible block of the current. Similar results were obtained with extracellular solutions containing 10 mM Ca^{2+} instead of the normal 1·5 mM, whereas removal of external Ca^{2+} caused an almost twofold increase of the current (Fig. 9*C*). To investigate whether this non-selective pathway is permeable to Ca^{2+}, we used external solutions containing 120 mM $NMDG^+$ and 20 mM Ca^{2+}. The addition of Ca^{2+} caused a shift of the reversal potential to less negative values, but this shift was apparently due to a block of the outward currents rather than to Ca^{2+} influx (Fig. 9*D*). Gd^{3+} (200 μM) did not significantly reduce the background current. Blocking effects of the different substances measured at −80 mV are summarized in Fig. 9*E*.

Electrogenesis

Having identified three different conductances in CPAE cells, we were interested in how modulation of these conductances affects the membrane potential. Figure 10*A* shows the effect of 100 μM Ba^{2+}, which completely blocks the inwardly rectifying K^+ currents, on the membrane potential of two different cells under current clamp. Note how the cell with an intermediately hyperpolarized membrane potential (−64 mV) was rapidly and reversibly depolarized to around −10 mV, whereas the membrane potential of the depolarized cell (−15 mV) was not affected. Membrane potentials from twenty-one cells before and after superfusion with 100 μM Ba^{2+} are summarized in Fig. 10*B*. The mean membrane potential changed from −29 ± 5 to −15 ± 2 mV. It should be noted that only the cells with membrane potentials more negative than −35 mV are depolarized, indicating that only in these cells the membrane potential is dependent on the inwardly rectifying K^+ channels.

Figure 10*C* shows a typical experiment in which a current-clamped cell (membrane potential = −15 mV) was superfused with a hypertonic solution (100 mM mannitol) and with a solution containing 500 μM quinine. The cell was reversibly depolarized to around −3 mV by both treatments, due to the inhibition of the volume-sensitive Cl^- current. In contrast, cells with membrane potentials more negative than the reversal potential for chloride were hyperpolarized by hypertonic cell shrinkage (Fig. 10*D*). These findings indicate that the volume-sensitive Cl^- conductance has a significant influence on the resting membrane potential. This was confirmed in experiments where we used a pipette solution containing 12 mM Cl^- instead of the normal 42 mM

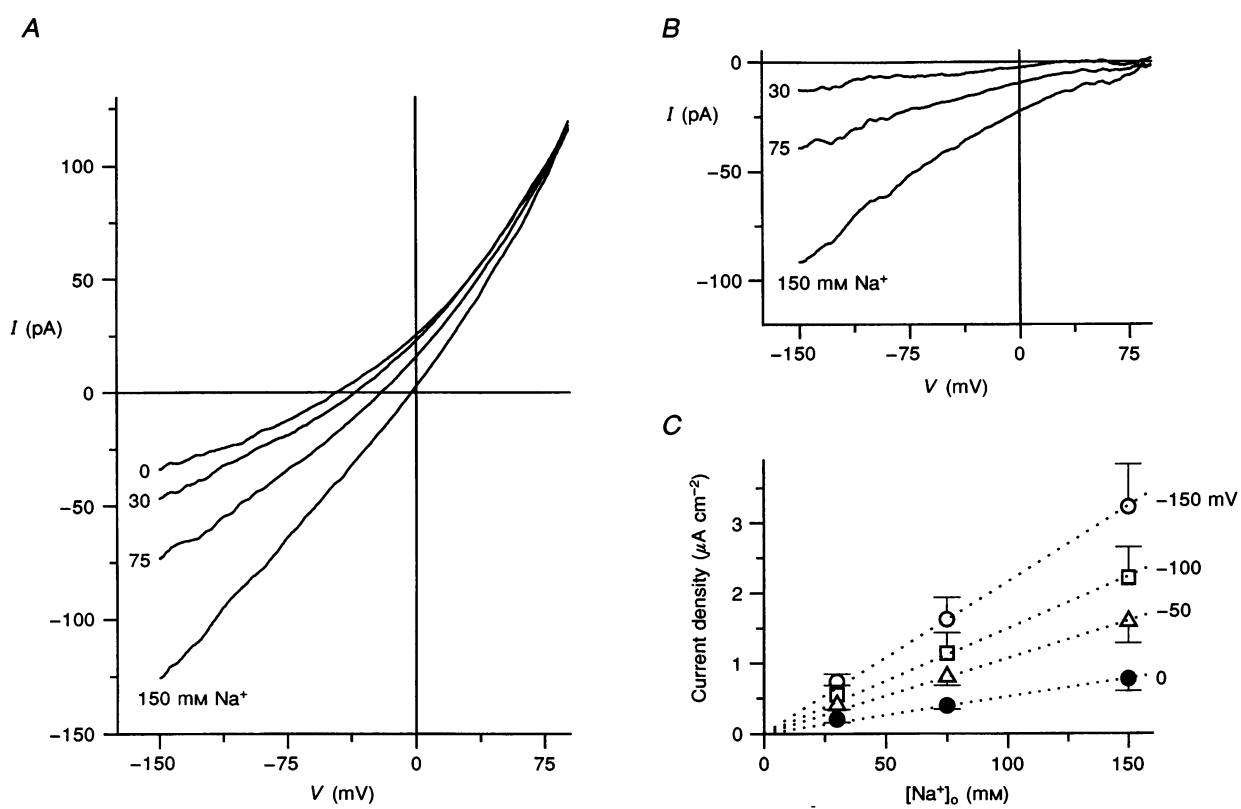

Figure 6. The inward current is proportional to the external Na^+ concentration

A, current–voltage relations measured in K^+-free hypertonic solution containing 150, 75, 30 or 0 mM Na^+. *B*, current–voltage relations obtained by subtracting currents measured in Na^+-free solution from those measured in the Na^+-containing solutions, representing inward Na^+ currents at different external Na^+ concentrations. *C*, inward currents with different extracellular Na^+ concentrations were measured at −150 mV (○), −100 mV (□), −50 mV (△) and 0 mV (●) normalized to membrane surface area, and data points for each potential were fitted by a straight line through the origin ($n = 5$).

($E_{Cl} = -66$ mV). The membrane potential of these cells, measured 5 min after obtaining the whole-cell configuration, was -62 ± 5 mV ($n = 7$), which is significantly more hyperpolarized than the control value (26 ± 3 mV, $n = 104$).

It is widely accepted that the membrane potential in resting endothelial cells is mainly determined by K^+ ions. However, our present results show that resting CPAE cells possess a Cl^--permeable volume-sensitive pathway and a Na^+-permeable, non-selective pathway, resulting in membrane potentials that often deviate substantially from the reversal potential for K^+ ($E_K = -83$ mV). This suggests that the membrane potentials of these cells tend to hyperpolarize towards E_K when the Cl^- and Na^+ components are eliminated. This is illustrated in Fig. 10*E*. A depolarized cell (membrane potential = −9 mV) is first superfused with a solution containing the non-permeable $NMDG^+$ instead of Na^+, causing a fast hyperpolarization. Subsequent hypertonicity causes a further hyperpolarization to potentials very near E_K. Note the oscillations of the membrane potential after superfusion with the Na^+-free solution. Such oscillations were frequently observed in the potential region between −40 and −60 mV. Membrane potentials from sixteen cells before and after superfusion with the Na^+-free, hypertonic solution are summarized in Fig. 10*F*. The mean membrane potential changed significantly from -28 ± 7 to -81 ± 2 mV.

DISCUSSION

The aim of this study was to describe the different membrane conductances that contribute to the resting potential in endothelial cells. Our results prove that resting CPAE cells possess at least three distinct membrane currents: an inwardly rectifying K^+ current, a volume-sensitive Cl^- current and a non-selective cation current.

Various properties of endothelial inwardly rectifying K^+ currents have been described in recent reports, such as a single-channel conductance between 20 and 30 pS, inhibition by micromolar concentrations of Ba^{2+} (von Beckerath *et al.* 1996), modulation by histamine (Nilius *et al.* 1993) and by G protein modulators (Pasyk, Cipris & Daniel., 1996). Our present results provide evidence for a Na^+-dependent inactivation mechanism, resembling the voltage-dependent block by external Na^+ as has been demonstrated previously in other cells (Ohmori, 1978; Standen & Stanfield, 1978; Biermans, Vereecke & Carmeliet, 1987). Quinidine and quinine exert a subunit-specific block of inwardly rectifying K^+ channels, which has been proposed to be useful in distinguishing between the quinidine-sensitive channels, like IRK1 and BIR11 (EC_{50} of 0·7 mM), and the quinidine-insensitive channels, like ROMK1 and BIR10 (less than 30% inhibition with 1 mM quinidine) (Doi *et al.* 1995). The observed block of about 20% of the inwardly rectifying K^+ currents in CPAE cells is in accordance with the expression of quinidine-insensitive K^+ channels.

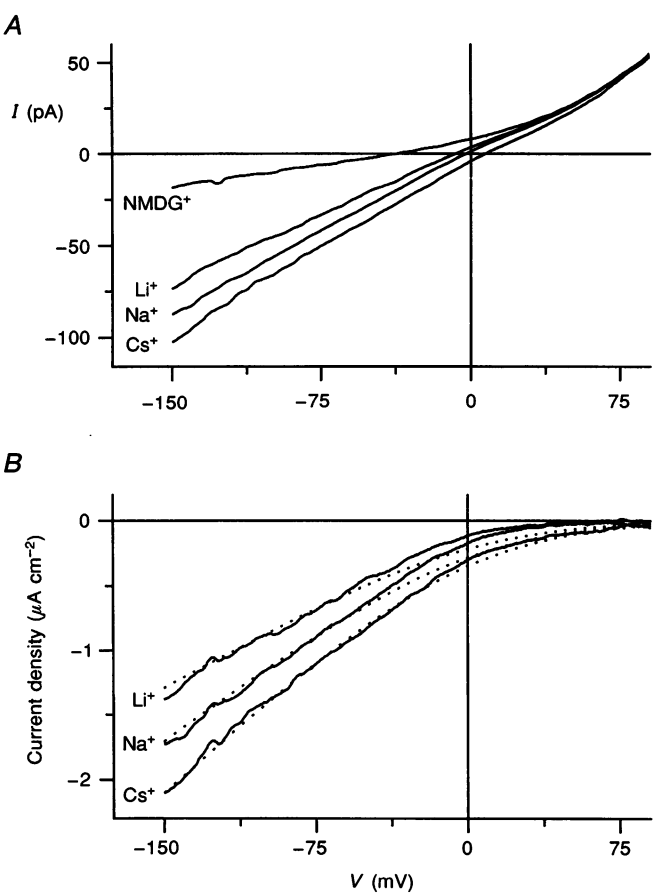

Figure 7. Cation selectivity of the Na^+-dependent background current

A, current–voltage relations measured in K^+-free hypertonic solutions containing 150 mM $NMDG^+$, Li^+, Na^+ or Cs^+. *B*, normalized inward currents for the different cations obtained by subtracting currents measured in $NMDG^+$ solution and dividing by membrane surface area. The dotted lines represent best fits using eqn (1). The pipette solution contained 10 mM BAPTA instead of 0·1 mM EGTA to buffer intracellular Ca^{2+}.

Volume-sensitive Cl^- currents under isotonic conditions have been described in rabbit atrial myocytes (Duan, Fermini & Nattel, 1995) and human peripheral T lymphocytes (Schumacher, Sakellaropoulos, Phipps & Schlichter, 1995). We also observed a Cl^- conductance under isotonic conditions that could be inhibited by cell shrinkage. This volume sensitivity, the moderate outward rectification and sensitivity to NPPB, quinine and quinidine suggest that this current is identical to the previously described volume-activated chloride current in endothelial cells (Nilius *et al.* 1994; Szücs, Buyse, Eggermont, Droogmans & Nilius, 1996; Voets, Droogmans & Nilius, 1996). Its presence under isotonic conditions could raise the question of whether it is activated by volume changes which occurred when transferring the cells from the growth medium to the normal bath solution or by the contact of the cell with the patch pipette. However, this Cl^- current was still present 3 h after the cells were transferred to the normal bath solution and >15 min after breaking into the cell with the normal pipette solution, which has a ~10% lower osmolality than the bath solution. We therefore assume that a volume-sensitive background Cl^- current is activated in CPAE cells under isotonic conditions, which can be enhanced by cell swelling induced by hypotonic solutions.

Our results give evidence for the presence of a non-selective cation current in resting CPAE cells. The linear current–voltage relation, $Cs^+ > Na^+ > Li^+ \gg NMDG^+$ selectivity and sensitivity for divalent cations resemble the properties of the background current described in rabbit sino-atrial node cells, rabbit atrial myocytes and human atrial myocytes (Hagiwara, Irisawa, Kasanuki & Hosoda, 1992; Crumb, Pigott & Clarckson, 1995). A non-selective cation current with a similar permeability sequence has been described in guinea-pig endocardial endothelial cells. This pathway was efficiently blocked by Gd^{3+} ($EC_{50} = 3{\cdot}1$ μM) and showed some permeability to Ca^{2+} (Manabe, Takano & Noma, 1995). In contrast, the non-selective cation current in CPAE cells was only marginally affected by 200 μM Gd^{3+}, and we have no evidence that it is Ca^{2+} permeable. In Na^+-free external solution Ca^{2+} blocked outward currents rather than inducing inward currents. However, membrane currents in the range of 1 pA, as described for store depletion-activated Ca^{2+}

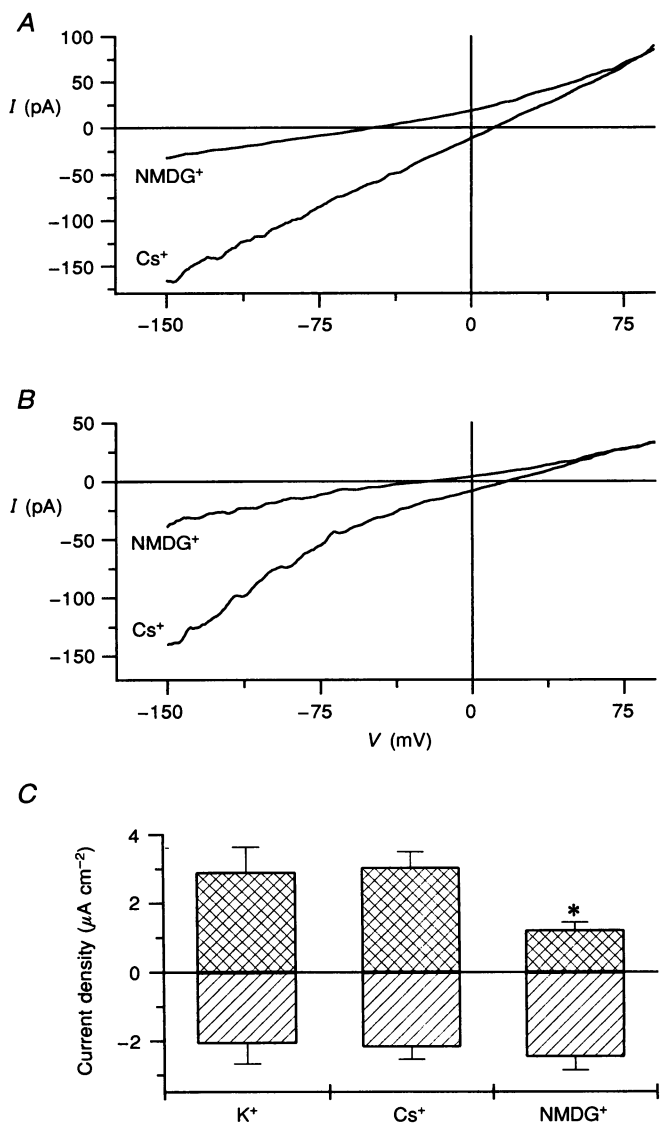

Figure 8. The outward component of the background current is cation dependent

A, current–voltage relations measured in K^+-free hypertonic solutions containing 150 mM Cs^+ or $NMDG^+$. The pipette solution contained 10 mM BAPTA and Cs^+ instead of K^+. *B*, same as *A* but the pipette solution contained $NMDG^+$ instead of K^+. *C*, the amplitudes of the currents measured in the 150 mM Cs^+ containing external solution with pipette solutions containing K^+ (control), Cs^+ or $NMDG^+$ were measured at ±100 mV and normalized to membrane surface area ($n = 5$ or more for each condition). * Significantly different from control.

entry in endothelial cells (Oike, Gericke, Droogmans & Nilius, 1994), fall below the detection limit of the whole-cell recordings and a limited Ca^{2+} permeability cannot be excluded. Therefore, the physiological role of this non-selective pathway is not clear. Under physiological conditions K^+ is the major intracellular and Na^+ the major extracellular cation. The non-selective conductance thus provides a small but permanent pathway for Na^+ influx and K^+ efflux.

Reported resting membrane potentials for different types of vascular endothelial cells seem to vary widely, with average values ranging between −25 and −77·5 mV (Colden-Standfield, Schilling, Ritchie, Eskin, Navarro & Kunze, 1987; Johns, Lategan, Lodge, Ryan, Van Breemen & Adams, 1987; Bregestovski, Bakhramov, Danilov, Moldobaeva & Takeda, 1988; Mehrke *et al.* 1991; Chen & Cheung, 1992; Marchenko & Sage, 1993; Baron, Frieden, Chabaud & Beny, 1996; Vaca, Licea & Possani, 1996). Here we report a bimodal distribution of resting membrane potential in CPAE cells, with peaks around −15 and −81 mV and a mean of −26 mV. A similar bimodal distribution has been described in bovine aortic endothelial cells (Mehrke *et al.* 1991).

About 30% of the tested cells were significantly depolarized when superfused with 100 μM Ba^{2+}, indicating that the outward part of the inwardly rectifying K^+ conductance is an important determinant of their membrane potential. The outward currents through inwardly rectifying K^+ channels reach a maximum at around −70 mV and tend to zero at more depolarized potentials, due to a rectification mechanism that may be intrinsic or Mg^{2+} dependent (Silver & DeCoursey, 1990; Elam & Lansman, 1995). Whenever inward currents through volume-sensitive Cl^- channels and non-selective cation channels exceed these outward K^+ currents, the membrane is depolarized to potentials between the reversal potentials for the chloride and the non-selective cation currents (> −30 mV). This is the case in the majority of the tested cells (69%), and a block of the inwardly rectifying

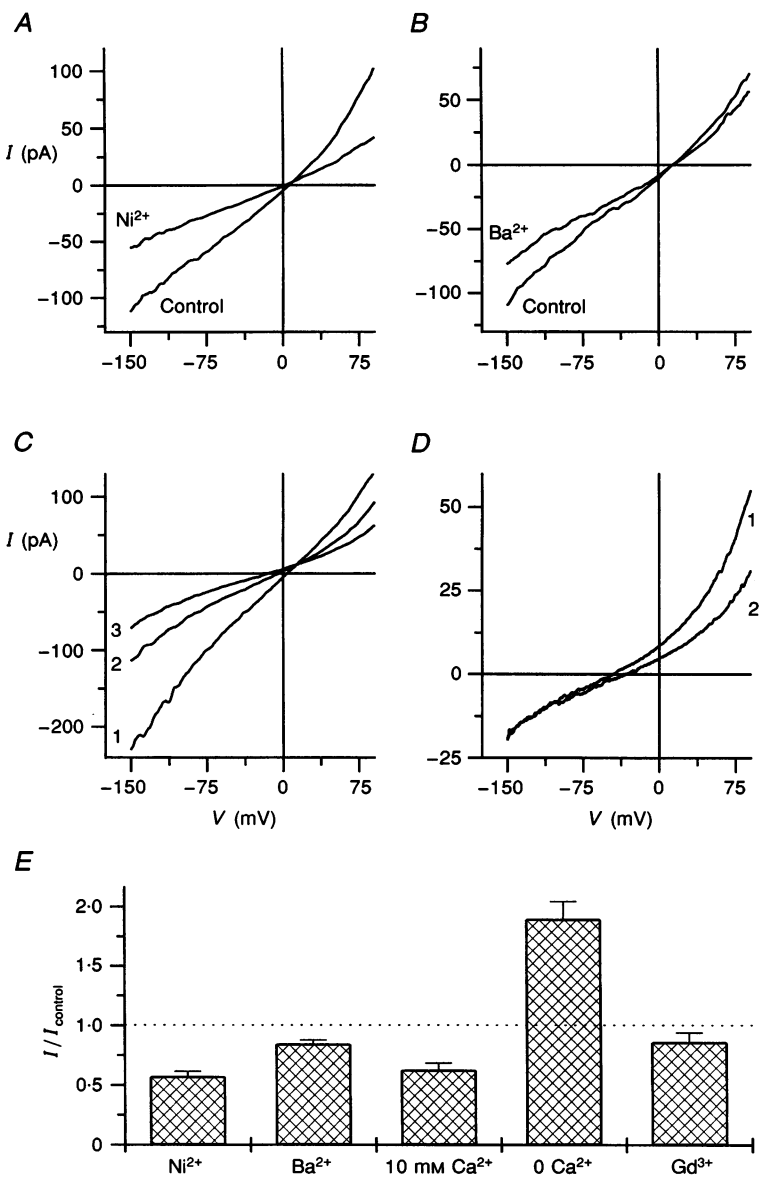

Figure 9. Blockade of the background current

Current–voltage relations showing the effect of 2 mM Ni^{2+} (*A*) or 2 mM Ba^{2+} (*B*) on background currents measured in K^+-free hypertonic solutions containing 150 mM Cs^+. *C*, effect of extracellular Ca^{2+} on background currents: nominally Ca^{2+} free (trace 1), 1·5 mM Ca^{2+} (trace 2) or 10 mM Ca^{2+} (trace 3). *D*, currents measured in Na^+-free extracellular solution (150 mM $NMDG^+$, trace 1) and in high-Ca^{2+}, Na^+-free solution (120 mM $NMDG^+$ and 20 mM Ca^{2+}, trace 2). *E*, the effect of the different compounds on the background current measured at −80 mV ($n = 4$ for each condition). The concentrations used were 2 mM (Ni^{2+} and Ba^{2+}), 0 mM and 10 mM (Ca^{2+}) and 200 μM (Gd^{3+}). Pipette solution contained 10 mM BAPTA.

K^+ conductance with Ba^{2+} has no significant effect on their membrane potentials.

The sum of the three different conductances results in a region between −70 and 0 mV with relatively small membrane currents and a low slope conductance, as has been described in many other endothelial cell types (Colden-Stanfield *et al.* 1987; Cannell & Sage, 1989; Fransen *et al.* 1995). As a consequence, the opening or closing of only a small number of channels can be sufficient to cause large membrane depolarizations or hyperpolarizations. This explains, at least partially, the observed large scattering of the resting membrane potentials and the occurrence of membrane potential oscillations.

A factor that may account for some of the differences in membrane potentials between different types of endothelial cells is the presence or absence of Ca^{2+}-activated K^+ channels. These channels, which are responsible for the observed membrane hyperpolarization after agonist-induced Ca^{2+} increase in intracellular in bovine aortic endothelial cells (Vaca *et al.* 1996) and pig coronary artery endothelial cells (Baron *et al.* 1996), could not be detected in CPAE cells (the authors' unpublished observations).

It should be noted that the experimental conditions under which endothelial membrane potentials were measured differ substantially between the different studies. We have shown that lowering the Cl^- concentration in the pipette can result in significantly more negative membrane potentials. In other studies, intracellular Cl^- concentrations were used between 5 and 150 mM. Such differences in experimental conditions should be taken into account when comparing the reported resting potentials.

The scattering of membrane potentials might also reflect different stages in the cell cycle, as has been described for several other types of proliferating cells (Kiefer *et al.* 1980; Boonstra *et al.* 1981; Wonderlin *et al.* 1995). We previously described an inhibition of endothelial cell proliferation by blockers of the volume-activated chloride channel, including quinine and NPPB (Voets, Szücs, Droogmans & Nilius, 1995). We show here that a volume-sensitive Cl^- current is present in non-swollen cells, with a smaller amplitude but

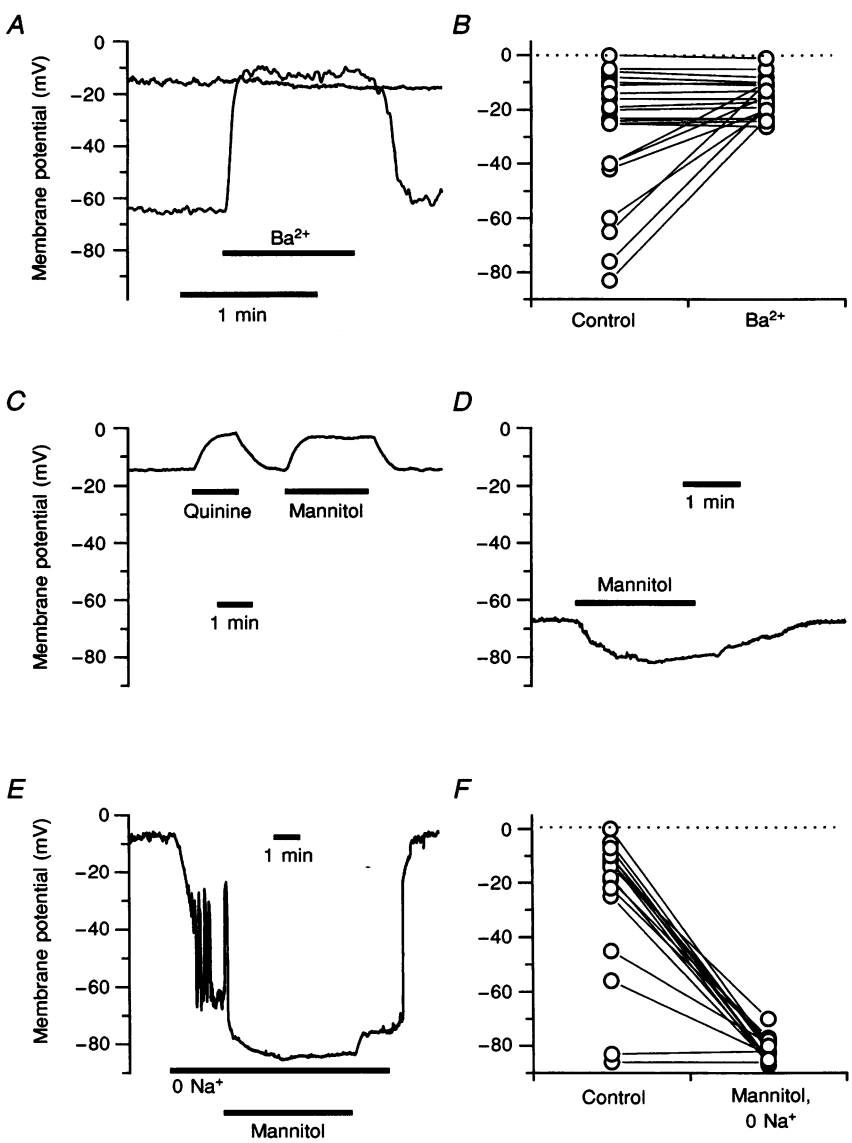

Figure 10. Modulation of the membrane potential

A, current-clamp recordings from two different cells showing the effect of 100 μM Ba^{2+} on the membrane potential. *B*, membrane potentials from 21 cells in normal Krebs solution and in Krebs solution containing 100 μM Ba^{2+}. *C*, current-clamp recordings from a single depolarized cell showing the effect of quinine (500 μM) and hypertonicity (100 mM mannitol) on the membrane potential. *D*, current-clamp recordings from a single intermediately polarized cell showing the effect of hypertonicity (100 mM mannitol) on the membrane potential. *E*, current-clamp recordings from a single depolarized cell showing the combined effect of a Na^+-free solution and hypertonicity (100 mM mannitol). *F*, membrane potentials from 16 cells in normal Krebs solution and in hypertonic Na^+-free solution.

similar sensitivity to NPPB, quinine and quinidine as the volume-activated current. It is possible that changes in cell volume during the cell cycle influence this volume-sensitive Cl^- current and hence regulate the membrane potential. If this is the case, a block of the volume-sensitive Cl^- current will strongly disturb this regulatory mechanism, which might eventually lead to a slower proliferation rate.

Adams, D. J., Barakeh, J., Laskey, R. & van Breemen, C. (1989). Ion channels and regulation of intracellular calcium in vascular endothelial cells. *FASEB Journal* **3**, 2389–2400.

Baron, A., Frieden, M., Chabaud, F. & Beny, J.-L. (1996). Ca^{2+}-dependent non-selective cation and potassium channels activated by bradykinin in pig coronary artery endothelial cells. *Journal of Physiology* **493**, 691–706.

Beny, J. L. & Pacicca, C. (1994). Bidirectional electrical communication between smooth muscle and endothelial cells in pig coronary artery. *American Journal of Physiology* **266**, H1465–1472.

Biermans, G., Vereecke, J. & Carmeliet, E. (1987). The mechanism of the inactivation of the inward-rectifying K current during hyperpolarizing steps in guinea-pig ventricular myocytes. *Pflügers Archiv* **410**, 604–613.

Boonstra, J., Mummery, C. L., Tertoolen, L. G., van der Saag, P.T. & De Laat, S. W. (1981). Cation transport and growth regulation in neuroblastoma cells. Modulations of K^+ transport and electrical membrane properties during the cell cycle. *Journal of Cellular Physiology* **107**, 75–83.

Bregestovski, P., Bakhramov, A., Danilov, S., Moldobaeva, A. & Takeda, K. (1988). Histamine-induced inward currents in cultured endothelial cells from human umbilical vein. *British Journal of Pharmacology* **95**, 429–436.

Cannell, M. B. & Sage, S. O. (1989). Bradykinin-evoked changes in cytosolic calcium and membrane currents in cultured bovine pulmonary artery endothelial cells. *Journal of Physiology* **419**, 555–568.

Chen, G. F. & Cheung, D. W. (1992). Characterization of acetylcholine-induced membrane hyperpolarization in endothelial cells. *Circulation Research* **70**, 257–263.

Colden-Stanfield, M., Schilling, W. P., Ritchie, A. K., Eskin, S. G., Navarro, L. T. & Kunze, D. L. (1987). Bradykinin-induced increases in cytosolic calcium and ionic currents in cultured bovine aortic endothelial cells. *Circulation Research* **61**, 632–640.

Crumb, W. J. Jr, Pigott, J. D. & Clarkson, C. W. (1995). Description of a nonselective cation current in human atrium. *Circulation Research* **77**, 950–956.

Daut, J., Standen, N. B. & Nelson, M. T. (1994). The role of the membrane potential of endothelial and smooth muscle cells in the regulation of coronary blood flow. *Journal of Cardiovascascular Electrophysiology* **5**, 154–181.

Davies, F. P., Olesen, S.-P., Clapham, D. E., Morrel, E. M. & Schoen, F. J. (1988). Endothelial communication. *Hypertension* **11**, 563–572.

Doi, T., Fakler, B., Schultz, J. H., Ehmke, H., Brandle, U., Zenner, H. P., Sussbrich, H., Lang, F., Ruppersberg, J. P. & Busch, A. E. (1995). Subunit-specific inhibition of inward-rectifier K^+ channels by quinidine. *FEBS Letters* **375**, 193–196.

Duan, D., Fermini, B. & Nattel, S. (1995). Alpha-adrenergic control of volume-regulated Cl^- currents in rabbit atrial myocytes. Characterization of a novel ionic regulatory mechanism. *Circulation Research* **77**, 379–393.

Elam, T. R. & Lansman, J. B. (1995). The role of Mg^{2+} in the inactivation of inwardly rectifying K^+ channels in aortic endothelial cells. *Journal of General Physiology* **105**, 463–484.

Fransen, P. F., Demolder, M. J. & Brutsaert, D. L. (1995). Whole cell membrane currents in cultured pig endocardial endothelial cells. *American Journal of Physiology* **268**, H2036–2047.

Graier, W. F., Sturek, M. & Kukovetz, W. R. (1994). Ca^{2+} regulation and endothelial vascular function. *Endothelium* **1**, 223–236.

Hagiwara, N., Irisawa, H., Kasanuki, H. & Hosoda, S. (1992). Background current in sino-atrial node cells of the rabbit heart. *Journal of Physiology* **448**, 53–72.

Hille, B. (1992). *Ionic Channels of Excitable Membranes.* Sinauer Associates, Sunderland, MA, USA.

Johns, A., Lategan, T. W., Lodge, N. J., Ryan, U. S., van Breemen, C. & Adams, D. J. (1987). Calcium entry through receptor-operated channels in bovine pulmonary artery endothelial cells. *Tissue and Cell* **19**, 733–745.

Kiefer, H., Blume, A. J. & Kaback, H. R. (1980). Membrane potential changes during mitogenic stimulation of mouse spleen lymphocytes. *Proceedings of the National Academy of Sciences of the USA* **77**, 2200–2204.

Manabe, K., Takano, M. & Noma, A. (1995). Non-selective cation current of guinea-pig endocardial endothelial cells. *Journal of Physiology* **487**, 407–419.

Marchenko, S. M. & Sage, S. O. (1993). Electrical properties of resting and acetylcholine-stimulated endothelium in intact rat aorta. *Journal of Physiology* **462**, 735–751.

Mehrke, G., Pohl, U. & Daut, J. (1991). Effects of vasoactive agonists on the membrane potential of cultured bovine aortic and guinea-pig coronary endothelium. *Journal of Physiology* **439**, 277–299.

Nilius, B., Schwarz, G. & Droogmans, G. (1993). Modulation by histamine of an inwardly rectifying potassium channel in human endothelial cells. *Journal of Physiology* **472**, 359–371.

Nilius, B., Sehrer, J. & Droogmans, G. (1994). Permeation properties and modulation of volume-activated Cl^--currents in human endothelial cells. *British Journal of Pharmacology* **112**, 1049–1056.

Ohmori, H. (1978). Inactivation kinetics and steady-state current noise in the anomalous rectifier of tunicate egg cell membranes. *Journal of Physiology* **281**, 77–99.

Oike, M., Gericke, M., Droogmans, G. & Nilius, B. (1994). Calcium entry activated by store depletion in human umbilical vein endothelial cells. *Cell Calcium* **16**, 367–376.

Pasyk, E. A., Cipris, S. & Daniel, E. E. (1996). A G protein, not cyclic AMP, mediates effects of VIP on the inwardly rectifying K^+ channels in endothelial cells. *Journal of Pharmacology and Experimental Therapeutics* **276**, 690–696.

Rhodin, J. A. (1967). The ultrastructure of mammalian arterioles and precapillary sphincters. *Journal of Ultrastructure Research* **18**, 181–223.

Schumacher, P. A., Sakellaropoulos, G., Phipps, D. J. & Schlichter, L. C. (1995). Small-conductance chloride channels in human peripheral T lymphocytes. *Journal of Membrane Biology* **145**, 217–232.

SILVER, M. R. & DECOURSEY, T. E. (1990). Intrinsic gating of inward rectifier in bovine pulmonary artery endothelial cells in the presence or absence of internal Mg^{2+}. *Journal of General Physiology* **96**, 109–133.

STANDEN, N. B. & STANFIELD, P. R. (1978). A potential- and time-dependent blockade of inward rectification in frog skeletal muscle fibres by barium and strontium ions. *Journal of Physiology* **280**, 169–191.

SZÜCS, G., BUYSE, G., EGGERMONT, J., DROOGMANS, G. & NILIUS, B. (1996). Characterization of volume-activated chloride currents in endothelial cells from bovine pulmonary artery. *Journal of Membrane Biology* **149**, 189–197.

VACA, L., LICEA, A. & POSSANI, L. D. (1996). Modulation of cell membrane potential in cultured vascular endothelium. *American Journal of Physiology* **270**, C819–824.

VOETS, T., DROOGMANS, G. & NILIUS, B. (1996). Potent block of volume-activated chloride currents in endothelial cells by the uncharged form of quinine and quinidine. *British Journal of Pharmacology* **118**, 1869–1871.

VOETS, T., SZÜCS, G., DROOGMANS, G. & NILIUS, B. (1995). Blockers of volume-activated Cl^- currents inhibit endothelial cell proliferation. *Pflügers Archiv* **431**, 132–134.

VON BECKERATH, N., DITTRICH, M., KLIEBER, H.-G. & DAUT, J. (1996). Inwardly rectifying K^+ channels in freshly dissociated coronary endothelial cells from guinea-pig heart. *Journal of Physiology* **491**, 357–365.

WONDERLIN, W. F., WOODFORK, K. A. & STROBL, J. S. (1995). Changes in membrane potential during the progression of MCF-7 human mammary tumor cells through the cell cycle. *Journal of Cellular Physiology* **165**, 177–185.

Acknowledgements

This work was supported by a grant from the Belgian Nationaal fonds voor Wetenschappelijk Onderzoek, NFWO (G0237995.N) to B.N. We thank Ms Anja Florizoone and Ms Marina Crabbé for their help with the cell cultures and Mr Jean Prenen for his assistance during the experiments.

Received 20 May 1996; accepted 30 July 1996.